Evidence for the interplanetary electric field effect on the OI 630.0 nm airglow over low latitude

D. Chakrabarty, R. Sekar, and R. Narayanan
Physical Research Laboratory, Ahmedabad, India

C. V. Devasia
Space Physics Laboratory, Vikram Sarabhai Space Center, Thiruvananthapuram, India

B. M. Pathan
Indian Institute of Geomagnetism, Navi Mumbai, India

Received 6 May 2005; revised 26 July 2005; accepted 1 August 2005; published 11 November 2005.

[1] On a geomagnetically disturbed and non-spread *F* night (12 February 2004), the OI 630.0 nm airglow intensity variations recorded from Gadanki (13.5°N, 79.2°E, dip 12.5°) reveal quasi-periodic intensity fluctuations superimposed on the large-scale temporal variation during 1945–2315 Indian Standard Time (IST, IST = Universal Time (UT) + 5.5 hours). The residual airglow intensity fluctuations (after detrending the large-scale variation) with periodicities of ~0.5 hours and ~1.0 hours, respectively, are found to vary in accordance with the *F* layer height variations over the dip equator as well as with the Y-component of the interplanetary electric field (IEF_y) variations calculated from the Advanced Composition Explorer (ACE) satellite data on 12 February 2004. Furthermore, these kind of periodic scale sizes in the residual airglow intensity fluctuations are not found on a geomagnetically quiet night (20 February 2004) and those intensity fluctuations do not show any correspondence with the *F* layer height variations over equator. Similar periodic components are also found in the temporal variations of instantaneous horizontal magnetic field (H) recorded at multiple stations over Indian subcontinent during the same interval on 12 February 2004. It is discussed that the currents responsible for the magnetic fluctuations are probably of magnetospheric origin. These observations using multiple techniques elicit the signature of the penetrating solar wind electric field in the nocturnal airglow intensity variations over low latitude during magnetically disturbed period.

Citation: Chakrabarty, D., R. Sekar, R. Narayanan, C. V. Devasia, and B. M. Pathan (2005), Evidence for the interplanetary electric field effect on the OI 630.0 nm airglow over low latitude, *J. Geophys. Res.*, *110*, A11301, doi:10.1029/2005JA011221.

1. Introduction

[2] During geomagnetic storm events, the low-latitude ionosphere, on occasions, is subjected to the interplanetary electric field (IEF) penetrating through the magnetosphere-ionosphere system. Using geomagnetic data from multiple stations and IMP-1 satellite data, *Nishida* [1968] was the first to systematically identify the coherence between the interplanetary magnetic field and the DP2 fluctuations. Thereafter, many important investigations [e.g., *Gonzales et al.*, 1979; *Fejer et al.*, 1979; *Reddy et al.*, 1979; *Kikuchi et al.*, 1996; *Sastri*, 2002] have revealed the connection between the equatorial and auroral electric field variations during geomagnetically disturbed conditions on the basis of magnetic and radar data obtained simultaneously from multiple stations. Recently, *Kelley et al.* [2003] have quantified the ratio of the dawn-to-dusk component of the IEF to the dawn-to-dusk electric field in the equatorial ionosphere by investigating a long-duration electric field penetration event captured by Jicamarca incoherent scatter radar. Although a number of investigations have been carried out to find out the signatures of IEF in the ionospheric *F* region over low latitudes, the effect of IEF on the thermospheric airglow emission over low latitudes has not been reported so far.

[3] OI 630.0 nm airglow photometry has long been recognized as a diagnostic tool in the investigation of ionospheric *F* region embedded in the terrestrial thermosphere. The *F* region processes have been studied using both ground-based [e.g., *Kulkarni and Rao*, 1972] and satellite-borne broadband photometers [e.g., *Chandra et al.*, 1973]. As of today, characteristic signatures in 630.0 nm nightglow intensity have been obtained corresponding to the

0148-0227/05/2005JA011221$09.00

F layer height variations [*Barbier*, 1959], nighttime reversal of the equatorial plasma fountain [e.g., *Sridharan et al.*, 1993], the midnight temperature anomaly [*Herrero and Meriwether*, 1980], and plasma depletions [e.g. *Sobral et al.*, 1980; *Mendillo and Baumgardner*, 1982] or enhancements [*Sekar et al.*, 2004] associated with equatorial spread *F* (ESF) events.

[4] It is well known that the equatorial ionospheric electric fields and the *F* region layer height get altered due to the penetration of IEF into low-latitude ionosphere during disturbed geomagnetic conditions. As the OI 630.0 nm airglow emission is anticorrelated with the *F* region layer height, it is generally expected that the effect of IEF may get registered in airglow intensity fluctuations. However, no direct evidence is available in the literature. Furthermore, the relationship between the fluctuating components in airglow intensity and the *F* region layer height variation is not known. In the present communication, it is shown that the quasi-periodic intensity fluctuations observed in OI 630.0 nm airglow over low latitude on a disturbed day are due to the fluctuations in the IEF.

2. Observations and Results

[5] The airglow observations which are reported in this communication have been made with the help of a narrow band (~3A°), narrow field of view (~3°) photometer operated to provide data with an average temporal resolution of ~2 min. The output of the detector is obtained in the form of photon count which is directly proportional to the intensity of airglow emission. It is pertinent here to mention that the calibration of this photometer with a standard light source is not essential as the present investigation deals only with the temporal variations of airglow intensity. The details on this photometer and the simultaneous observation of ESF from Gadanki by this photometer in conjunction with the MST radar have been reported earlier [*Sekar et al.*, 2004]. A coordinated campaign involving the MST radar and the photometer was conducted during 11–22 February 2004. In the present communication, optical observations pertaining to a geomagnetically disturbed night (12 February 2004; A_P = 30) and a quiet night(20 February 2004; A_P = 4) are reported.

2.1. Photometric and Ionosonde Measurements on 12 February 2004

[6] Figure 1 consists of three subplots pertaining to the observations on 12 February 2004. The abscissae for all the subplots are expressed in time in Indian Standard Time (IST = Universal Time (UT) + 5.5 hours). The topmost subplot (Figure 1a) depicts the OI 630.0 nm nightglow intensity (maximum measurement error in airglow is ~±400 counts) over Gadanki and the *F* layer peak height (h_PF_2) variations (maximum uncertainty in the height measurements is ~5 km) with 15 min temporal resolution over SHAR, a station 100 km east of Gadanki. The large-scale airglow intensity variation on this night is characterized by its monotonic increase till ~2130 IST followed by gradual decrease till the end of the observation. Small-scale (T_s) intensity fluctuations in the range of 0.25 hours $< T_s \leq$ 1.0 hour are discerned to be superimposed on the large-scale variation at regular intervals during the period of observation. The peak to peak amplitude of small-scale airglow intensity fluctuations varies from 8 to 10% of the background values and corresponds to 4 to 5 Rayleighs considering a typical value for the nocturnal 630.0 nm airglow intensity to be ~50 Rayleighs. The h_PF_2 variation over SHAR, on the other hand, was marked by monotonic decrease till ~2130 IST followed by steady increase till midnight. The smoothed airglow intensity curve plotted in Figure 1a (constructed by taking running average) which is devoid of the small-scale intensity fluctuations, is used to filter out the residual fluctuations in photon counts which is plotted in Figure 1c. The intermediate subplot (Figure 1b) depicts the h_PF_2 variations over Trivandrum (TRD), an equatorial station (8.68°N, 77.0°E, dip 0.5°N) during the same interval. It is noticed that the h_PF_2 variations over SHAR and TRD are, in general, similar on this night. Figure 1c illustrates the temporal variation of the residual photon counts, obtained after detrending the large-scale airglow intensity variation, along with the time rate of changes in h_PF_2 (dh_PF_2/dt) over TRD. It is noticed that the variabilities in dh_PF_2/dt (maximum propagation error in dh_PF_2/dt is ~±6 m/s) over TRD during 1945–2315 IST do have their counterparts in the temporal variabilities in the residual intensity variations. The time difference between the crests and troughs that appear to be mutually correspondent in the two time series is almost close to zero before ~2215 IST. However, during 2215–2315 IST, oscillations in dh_PF_2/dt over TRD seem to precede the airglow intensity oscillations by ~15 min which is of the order of the resolution of the available ionosonde data.

2.2. Photometric and Ionosonde Measurements on 20 February 2004

[7] Figure 2 is composed of three subplots (similar to those of Figure 1) corresponding to 20 February 2004. Figure 2a depicts the airglow intensity variation along with the h_PF_2 variations over SHAR. This subplot also reveals postevening increase in the airglow intensity (maximum measurement error in airglow is ~±450 counts) till ~2130 IST followed by decrease in the intensity similar to Figure 1a. However, small-scale intensity fluctuations observed on 12 February are absent on this night. The large-scale h_PF_2 variation over SHAR was also marked by the continual descent up to ~2130 IST followed by slow, gradual ascent similar to Figure 1a. However, Figures 2a and 2b reveal that large-scale h_PF_2 variations over SHAR and TRD are different on this night unlike Figure 1. Figure 2c shows that, unlike in Figure 1c, the temporal variations of the residual photon counts (mostly statistical fluctuations) are uncorrelated with dh_PF_2/dt over TRD.

2.3. Time Lag Between Ionospheric and ACE Satellite Measurements

[8] In order to verify that the fluctuations in h_PF_2 and airglow intensity during 1945–2315 IST on 12 February 2005 are due to penetrating disturbance electric field event, the dawn-to-dusk component of IEF was calculated based on the solar wind velocity and interplanetary magnetic field values measured by ACE satellite located at the Libration point L1(~1.41×10^6km from Earth). It is also important to calculate reasonably accurately the time delays which

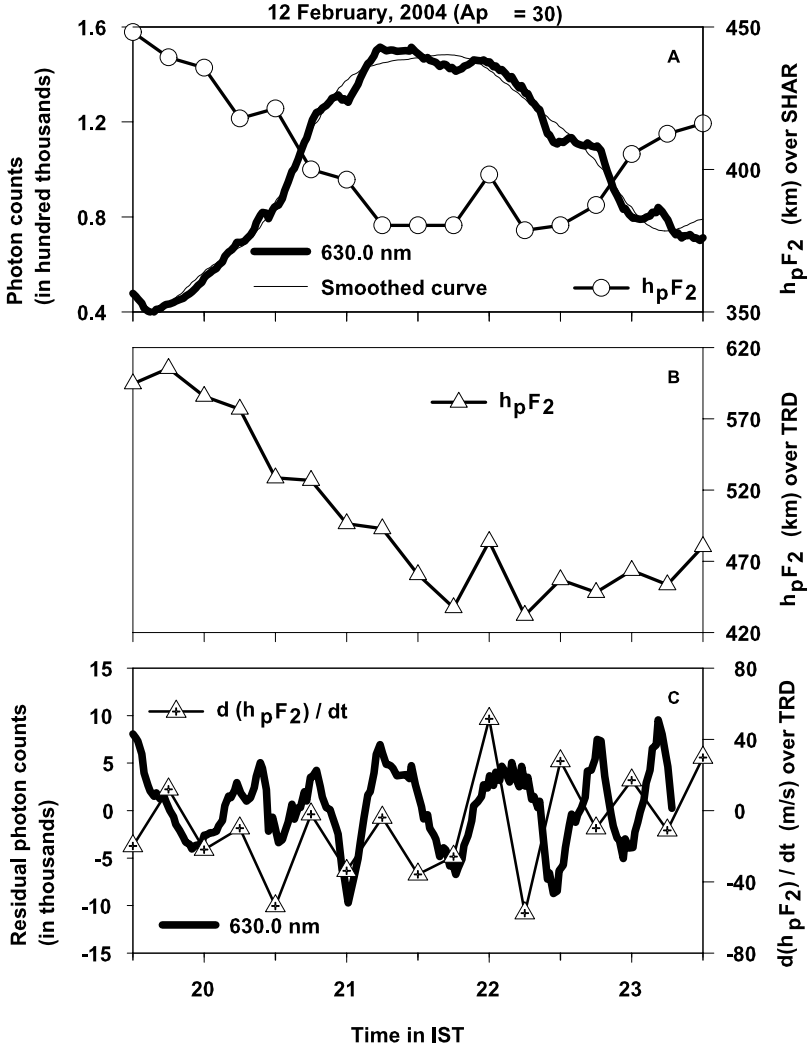

Figure 1. (a) 630.0 nm airglow intensity variations over Gadanki along with the h_PF_2 variations over SHAR on a geomagnetically disturbed night (12 February 2004; $A_P = 30$). The maximum measurement error in airglow is $\sim\pm400$ counts. Note the presence of small-scale airglow intensity variations on this night. Notice also the smoothed curve which is generated by taking suitable running average of the data points so that it is devoid of the small-scale intensity fluctuations. This curve is used to extract the intensity residuals. (b) h_PF_2 variations over Trivandrum (TRD) during the same interval. Uncertainty in the height measurements is $\sim$5 km. (c) Residual airglow intensity variation along with the time rate of change of h_PF_2 over TRD. The maximum propagation error in dh_PF_2/dt is $\sim\pm6$ m/s.

separate the satellite and ionospheric observations (for a comprehensive discussion, see *Ridley et al.* [1998]). The total time lag comprises of three components. The travel time of the solar wind from the spacecraft to the subsolar bow shock (t_1), propagation time from the bow shock to the magnetopause (t_2), and the Alfven transit time (t_3) along magnetic field lines from the subsolar magnetopause to the ionosphere. The magnetopause stand-off distance (X_{mp}), for the given period, is calculated based on the simple pressure balance equation between the solar wind dynamic pressure and the magnetospheric pressure [e.g., *Roelof and Sibeck*, 1993] using the proton number density (adjusted for helium content, noting the mass factor of 4) in the solar wind and the solar wind bulk velocity v (during this period, v varied from 645 km/s to 750 km/s). X_{mp} is found to vary between $\sim$10.92 R_E (R_E, the radius of the Earth, is taken as 6375 km) and $\sim$9.7 R_E during the interval under consideration here. The solar wind advection time t_1 is then calculated using the formula described by *Lester et al.* [1993].

$$t_1 = \frac{X_{sat} - X_{bs} + L\tan\phi}{v}, \tag{1}$$

where X_{sat} is the geocentric upstream distance of the spacecraft, X_{bs} is the geocentric distance to the subsolar bow shock and L is the orthogonal distance of the spacecraft from the Sun-Earth line. This calculation is based on the assumptions that the Earth-bound solar wind upstream of the bow shock is not accelerated, the solar wind "phase front" is at angle ϕ (lying within $\pm45°$) with the Sun-Earth line and the "phase front" is linear over scale sizes greater than L and the cross section of the magnetosphere. Using

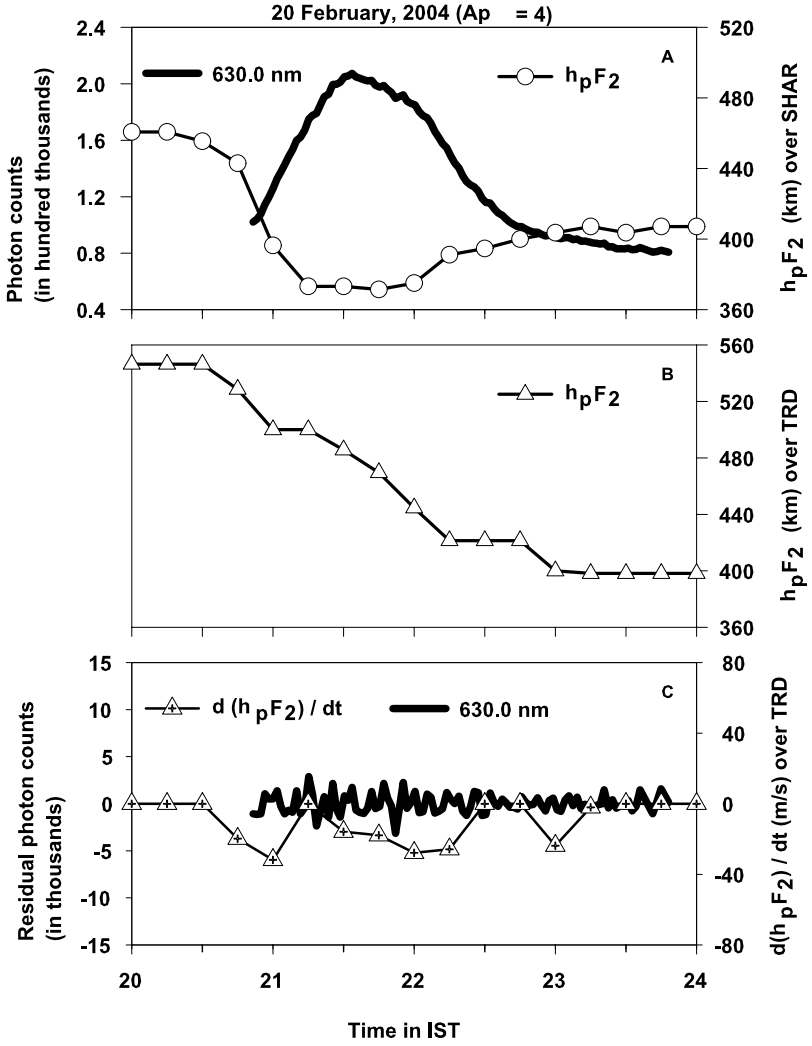

Figure 2. (a) The 630.0 nm airglow intensity variations over Gadanki along with the h_PF_2 variations over SHAR on a geomagnetically quiet night (20 February 2004; $A_P = 4$). The maximum measurement error in airglow is ~±450 counts. Note the absence of small-scale airglow intensity variations on this night. (b) The h_PF_2 variations over Trivandrum (TRD) during the same interval. (c) Residual airglow intensity variation along with the time rate of change of h_PF_2 over TRD.

the empirical model of *Peredo et al.* [1995], *Khan and Cowley* [1999] comprehensively analyzed the observed shock locations and found that a typical bow shock distance, X_{bs}, is, in general, 1.46 times the distance of the subsolar magnetopause. Using this multiplicative factor, X_{bs} is found to vary between ~16.59 R_E and ~14.56 R_E during the interval under consideration. *Khan and Cowley* [1999] also showed that the magnetosheath transit time t_2 can be derived using the gas dynamic model of *Spreiter and Stahara* [1980] as follows:

$$t_2 = \frac{1.66X_{mp}}{(v - 72)} \ln\frac{v}{72}. \quad (2)$$

It is to be noted here that t_2 can also be deduced from the model of *Spreiter and Stahara* [1980] by dividing the magnetosheath thickness with an average magnetosheath velocity (v_{avg}) which is assumed to fall off in an approximately linear fashion from $v_{avg}/4$ at the bow shock to zero at the magnetopause [e.g., see *Lester et al.*, 1993]. It is verified that the values of t_2 obtained by both the methods agree well in the present case.

[9] The average Alfven transit time, t_3, is taken as 2 min [*Khan and Cowley*, 1999]. The total time lag from the ACE spacecraft to the ionosphere is thus calculated by adding t_1, t_2, and t_3. The total time lag, in the present case, is found to range from ~48.7 min to ~42.1 min during the interval under consideration. The sources of uncertainties involved in this type of calculation are comprehensively discussed by *Ridley et al.* [1998] and *Khan and Cowley* [1999]. It is found that the maximum error in the present calculation is of the order of 5 min.

2.4. Intercomparison of the Time-Delayed IEF_y, Ionosonde, and Photometric Measurements on 12 February 2004

[10] The average temporal resolution of the airglow data is 120 s. However, ACE data used in the present study have

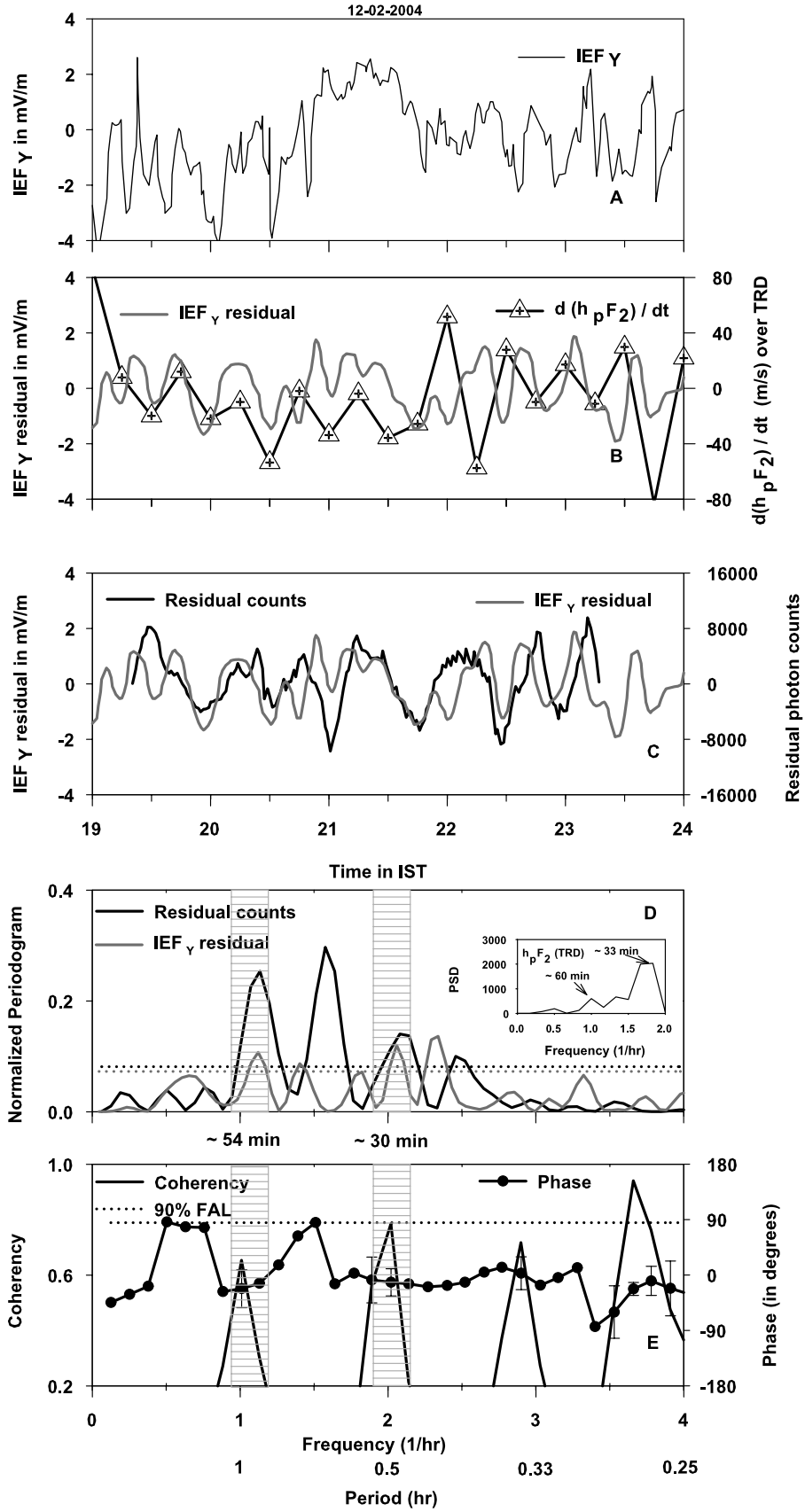
12-02-2004
IEF Y
IEF Y in mV/m
A
IEF Y residual
d (h pF2) / dt
IEF Y residual in mV/m
d(h pF2) / dt (m/s) over TRD
B
Residual counts
IEF Y residual
IEF Y residual in mV/m
Residual photon counts
C
Time in IST
Residual counts
IEF Y residual
D
PSD
hpF2 (TRD)
~ 33 min
~ 60 min
Frequency (1/hr)
Normalized Periodogram
~ 54 min
~ 30 min
Coherency
90% FAL
Phase
Coherency
Phase (in degrees)
E
Frequency (1/hr)
Period (hr)

Figure 3

64 s resolution. Therefore the y component of IEF, calculated from ACE data, is first subjected to a 2-point moving average scheme (low pass filtering). Thereafter, each IEF_y datum point is time shifted by the corresponding lag time from L1 to ionosphere. The filtered and time-shifted IEF_y values are then plotted in Figure 3a. The variation in IEF_y is subsequently subjected to Fourier domain filtering in which the frequency components less than 0.5 cycles/hour (periods >2 hours) are filtered off. This procedure automatically takes care of the detrending of the IEF_y data. The detrending of IEF_y data prevents leakage of spectral powers from the low-frequency components (frequency components less than 0.5 cycles/hour). Since the resolution of the h_PF_2 data is 15 min, frequency components more than 4 cycles/hour (periods <15 min) in IEF_y are also eliminated for useful comparison. The filtered data are subsequently reconstructed in the time domain. The resultant IEF_y residual time series, thus obtained, is compared with the dh_PF_2/dt variations over Thumba as well as with the residual photon counts in the Figures 3b and 3c, respectively. It is noticed that the IEF_y residuals agree reasonably well with dh_PF_2/dt variations as well as with residual counts except mainly ~2045 and ~2200 IST.

[11] As the time series of residual airglow and IEF_y residual are not strictly evenly sampled, a special harmonic analysis [*Schulz and Stattegger*, 1997] which can handle unevenly sampled data is followed to obtain frequency components. The harmonic analyses generate normalized periodograms from the residual (not normalized) time series. The spectral power contained in each spectral element is normalized with respect to the total power contained in all the spectral elements taken together. This procedure makes the relative distribution of the spectral power independent of the spectral windowing (to avoid spectral leakage) used in the algorithm. Both the normalized periodograms are depicted on the same scale in Figure 3d. "Significant" frequency components in both the time series exceed the critical level (marked by dotted lines) determined by Fisher's test. Therefore Figure 3d reveals the relative importance of each "significant" frequency component in the two time series. It is noticed from Figure 3d that the residuals of airglow counts and the IEF_y both have "significant" and common frequency components (marked by hatch in Figure 3d) at ~1 cycle/hour (period ~1.0 hour) and ~2 cycles/hour (period ~0.5 hour). Harmonic analysis of the evenly sampled, detrended (allowing the frequency pass-band 4.0–0.5 cycles/hour only) dh_PF_2/dt time series (shown in Figure 3b) is also carried out using a standard Fast Fourier Transform (FFT) algorithm and the power spectral densities (PSD, sum squared amplitudes) are shown as an inset of Figure 3d for comparison. As the number of dh_PF_2/dt data points are very limited, reliable estimation of the critical level is not possible. Nevertheless, it is clear that the frequency components close to 1 cycle/hour and 2 cycles/hour are also present in the dh_PF_2/dt time series.

[12] In order to find out whether the residual airglow intensity fluctuations are causally related to the fluctuations in IEF_y, a cross spectrum analysis is performed between the two residual time series (plotted and compared in Figure 3c) using a standard methodology [*Schulz and Stattegger*, 1997]. Cross spectrum analysis generates coherency and phase spectrum from the two residual (not normalized) time series. It is found that substantial coherency between the two time series exist (see Figure 3e) at frequencies ~3.7 cycles/hour (period ~0.27 hour), ~2.8 cycles/hour (period ~0.36 hour), ~2 cycles/hour (period ~0.5 hour) and ~1 cycle/hour (period ~1.0 hour). However, coherency at frequencies ~3.7 cycles/hour, ~2.8 cycles/hour are neglected owing to the absence of simultaneous "significant" spectral peaks in both the time series (see the normalized periodograms in Figure 3d). High degree of coherence (close to the false alarm level at 90%) is found (marked in Figure 3e) especially for the frequency component at ~2 cycles/hour. Coherency at the frequency component ~1 cycle/hour is also found (marked in Figure 3e) to be substantial (close to the false alarm level at 80% not shown in figure). Further, these two frequency components are simultaneously present and "significant" in both the IEF_y and airglow residual time series (see Figure 3d). The phase spectrum, which is overlaid on the coherency spectrum in Figure 3e, does not reveal any sharp changes around these two frequencies.

2.5. Horizontal Magnetic Field Measurements on 12 and 20 February 2004

[13] In order to investigate the differences, if any, in the variations of horizontal magnetic field (H) (during periods of airglow observations), H variations recorded from Tirunelveli (TIR, 8.67°N, 77.82°E, dip 1.86°), Pondicherry

Figure 3. (a) The time shifted (by the travel time from L1 to ionosphere) variations in the Y component of the Interplanetary Electric Field (thin black line) on 12 February, 2004, (b) comparison between the time rate of change of h_PF_2 over TRD (black line with legends) and the IEF_y residuals (grey line), (c) comparison between the residual airglow intensity variations (black line) and the IEF_y residuals (grey line), and (d) harmonic components in the airglow (black line) and the IEF_y residuals (grey line). Superimposed horizontal lines in black and grey denote the critical levels determined by the Fisher's test for the two time series. The power spectral densities (PSD) of the detrended dh_PF_2/dt variations are also shown as an inset. Notice the simultaneous presence of ~2 cycles/hour (period ~0.5 hour) and ~1 cycle/hour (period ~1.0 hour) frequency component in residual IEF_y, airglow (marked by hatch). Note also the presence of the same frequency components in dh_PF_2/dt (marked by arrow) time series. (e) Coherency and phase spectrum for the residual IEF_y, airglow time series. Dotted line indicates 90% false alarm level for the coherency spectrum. Note high degree of coherence at frequencies ~3.7 cycles/hour (period ~0.27 hour), ~2.8 cycles/hour (period ~0.36 hour), ~2 cycles/hour (period ~0.5 hour) and ~1 cycle/hour (period ~1.0 hour). Coherency at frequencies ~3.7 cycles/hour and ~2.8 cycles/hour are neglected owing to the absence of simultaneous "significant" spectral peaks in both the time series. The frequency components at ~2 cycles/hour and ~1 cycle/hour are characterized by high coherency and stable phase relationship.

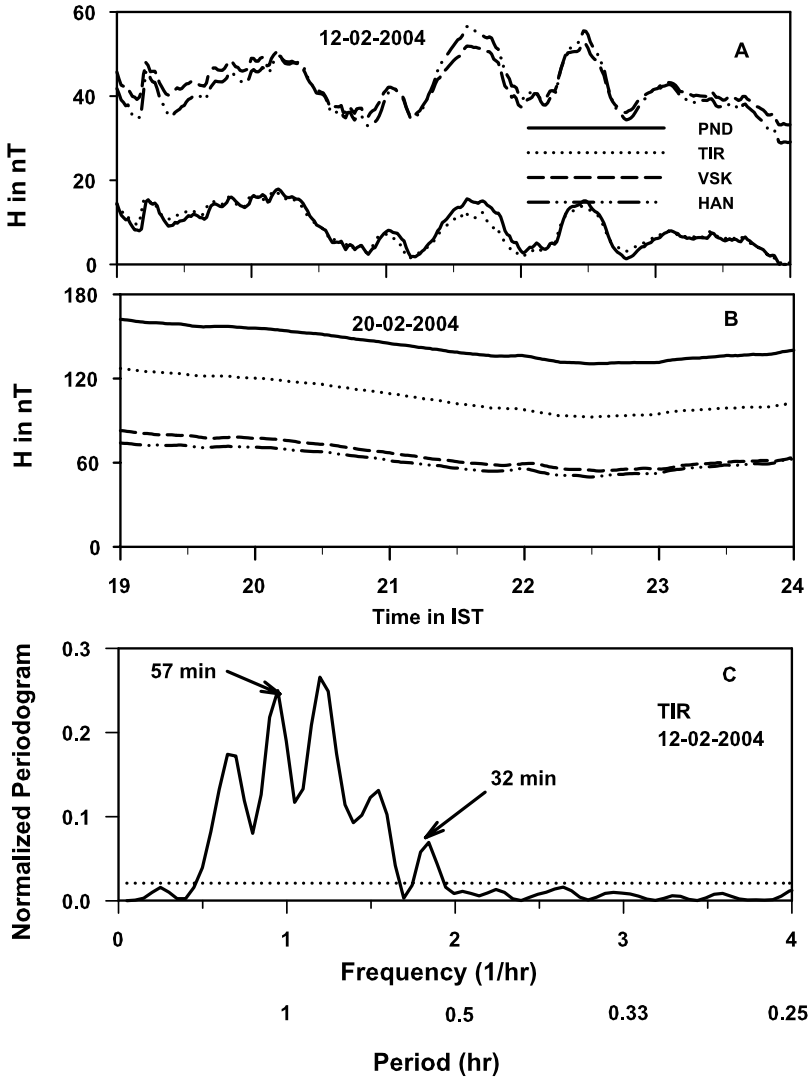

Figure 4. Horizontal magnetic field variations (H) recorded at Tirunelveli (TIR), Pondicherry (PND), Visakhapatnam (VSK), and Hanley (HAN) (a) on 12 February 2004 and on (b) 20 February 2004. The presence of in-phase, quasi-periodic fluctuations in H on 12 February 2004 is apparent in contrast with 20 February 2004. (c) Normalized periodograms for the detrended H variations recorded at Tirunelveli (H_{TIR}). Both the frequency components (marked by arrow) ~1 cycle/hour and ~2 cycles/hour are present in H.

(PND, 11.92°N, 79.92°E, dip 9.58°), Visakhapatnam (VSK, 17.67°N, 83.32°E, dip 22.6°), and Hanle (HAN, 32.77°N, 78.96°E, dip 50.03°) on 12 and 20 February 2004 are compared in Figures 4a and 4b, respectively. It is to be noted here that in the presence of oscillatory features in the temporal variations of H during the given interval on 12 February 2004, the nighttime representative base value is not subtracted from the instantaneous H values (unlike the method applicable for daytime to find out the ΔH for a given station). Figure 4a therefore depicts the temporal evolution of H values recorded at the four stations on 12 February, whereas Figure 4b depicts the same on 20 February 2004. It is apparent from the subplots that that magnetic fluctuations with seemingly multiple frequencies are present on 12 February 2004 during 1930–2330 IST, whereas 20 February 2004 is marked by the absence of them. The fluctuations in H are almost similar, simultaneous (without any appreciable time delay) and in phase over all the stations encompassing dip equator to station beyond S_q focus. It is also noticed, by comparing Figures 4a and 1c, that the fluctuations in H are anticorrelated with airglow fluctuations. In order to find the representative spectral components in H, the H variation recorded at TIR (H_{TIR}) is first detrended (by choosing a frequency pass-band 4.0–0.5 cycles/hr similar to IEF_y data with similar technique as described in detail in section 2.4). Normalized periodogram is generated for H_{TIR} which is shown in Figure 4c. Multiple frequency components including ~2 cycles/hour and ~1 cycle/hour are found to be present in the H_{TIR} time series. Furthermore, it is also noticed that the frequency component ~1 cycle/hour is more dominant compared to the ~2 cycles/hour compo-

nent in the *H* data. This is in contrast with the dh_PF_2/dt time series where the frequency component ~2 cycles/hour is found to be more dominant.

3. Discussion

[14] It is known that the OI 630.0 nm nocturnal airglow emission arises owing to the dissociative recombination of O_2^+ with ionospheric electrons. Descent/ascent of *F* layer height causes change in the concentrations of the constituents in the airglow emission altitude and therefore enhances/decreases the volume emission rate by creating favorable/unfavorable conditions for the dissociative recombination reaction. It is to be noted that the temporal variabilities in h_PF_2, which is the virtual height at 0.834 of f_oF_2 and a routinely scaled parameter, correspond to the temporal variabilities in the *F* peak height h_mF_2 and their values are known to agree well with each other [e.g., *Shirke*, 1963] especially during nighttime. Therefore the large-scale anticorrelation of airglow intensity variation with the h_PF_2 variations over SHAR in both Figures 1a and 2a is expected. It is to be noted that the h_PF_2 variations over SHAR are sensitive to both electric field and meridional wind variations whereas over TRD, h_PF_2 responds to only electric field variations [*Krishna Murthy et al.*, 1990]. Therefore the similarities in the large-scale temporal variations of h_PF_2 over SHAR and TRD on 12 February (Figures 1a and 1b, respectively), a geomagnetically disturbed night, are indicative of the active role played by electric field on that night even over SHAR. The large-scale h_PF_2 variations over SHAR on 20 February, an international quiet day, do not exhibit such similarities with the h_PF_2 variations over TRD (Figures 2a and 2b) bringing out the additional roles played by meridional wind in determining the h_PF_2 variations over SHAR.

[15] In the absence of any direct electric field measurements over Indian zone, dh_PF_2/dt over TRD during nighttime is taken as a "proxy" for the zonal electric field variation since the apparent vertical drift due to chemical loss process beyond 300 km is negligible [*Bittencourt and Abdu*, 1981; *Krishna Murthy et al.*, 1990]. Since on both 12 February (Figure 1) and 20 February (Figure 2), during the interval under consideration, the h_PF_2 heights did not go below 300 km, dh_PF_2/dt can be safely considered as a "proxy" for the zonal electric field variation. It is interesting to note that the small-scale variations in the observed airglow intensity and dh_PF_2/dt are directly correlated (Figure 1c) except during 2215–2315 IST. In order to understand the direct correlation between the airglow intensity and dh_PF_2/dt, the Barbier's relation [*Barbier*, 1959] is differentiated with respect to time. The differentiation provides a relationship between the temporal variation in the nocturnal 630.0 nm airglow intensity with two terms, one containing the changes in the *F* region peak electron density and the other containing the temporal changes in the peak layer height. The first term gains importance in the presence of large and rapid electron density changes like the plasma depletion events during ESF which is implicitly pointed out, for example, by *Sekar et al.* [2004]. As the observations reported here pertain to non-ESF nights, which are confirmed by the simultaneous Indian MST radar observations, the small-scale variations in the airglow intensity are unlikely to be associated with the changes in the electron density. This point is strengthened from the temporal variation of peak electron density (obtained from f_oF_2) on 12 February 2004 (not shown in figure) wherein no small-scale fluctuations are observed. The second term, which is inversely dependent on the exponential variation of the layer height and also directly dependent on the small-scale variation of the layer height, gains importance in this case. Therefore the direct correlation between the small-scale variations of layer height and airglow intensities is consistent with the Barbier's relation. The similarities in the temporal variations in the residual airglow intensity and the h_PF_2 over TRD in Figure 1c confirm the above proposition and adduce the electric field associated changes in the airglow intensity variations on this night during 1945–2315 IST. However, the reason for the time delay between the residual airglow intensity variations and dh_PF_2/dt variations during 2215–2315 IST is not clear and this aspect needs further investigation (Figure 1c).

[16] The overall similarities in the variations of dh_PF_2/dt and residual airglow intensity with residual IEF_y variations (Figures 3b and 3c, respectively) suggest that IEF_y acted as a common driver in bringing about the fluctuations in dh_PF_2/dt over TRD and as a consequence, in the residual airglow intensity over Gadanki on 12 February 2004. Figures 3d and 3e, in perspective with Figures 3b and 3c, bring out the two frequencies (~2 cycles/hour and ~1 cycle/hour) at which IEF affects the low-latitude ionosphere for the event under consideration. It is interesting to note that the similarities of IEF_y with residual airglow intensity and dh_PF_2/dt break down during ~2045 and 2200 IST (see Figures 3b and 3c) which are also the times when IEF_y changes its polarity (see Figure 3a).

[17] It is generally accepted that nighttime ionospheric conductivity is not large enough to support substantial ionospheric currents. As discussed by *Stening and Winch* [1987], the oscillatory features in the instantaneous *H* variations during nighttime are often caused by modulation in the ring current especially so during disturbed period. In the present case (see Figure 4), the presence of similar and simultaneous fluctuations in *H* recorded on 12 February 2004, at all the four stations spread over a vast latitudinal sector indicates that the magnetic fluctuations are probably caused by magnetospheric currents on this night. Further, the differences in the spectral components in *H* and dh_PF_2/dt also indirectly indicate that the magnetic field discussed here has different origin other than ionosphere. *Gonzales et al.* [1979] opined that the accuracy of correlations between nighttime *H* variations over dip equator, zonal electric field variations and the interplanetary magnetic field (IMF) variations during disturbed geomagnetic conditions, depends on the strength of the ring current. The strength of the ring current was relatively high (~−50 nT) in the present case. On the basis of the above discussion, the magnetic fluctuations on 12 February may be attributed to be of magnetospheric origin. However, the anticorrelation between the fluctuations in *H* and in airglow needs to be investigated further.

[18] The frequency dependence of the shielding between ionosphere and magnetosphere is extensively studied by *Earle and Kelley* [1987]. They, as well as *Gonzales et al.* [1979], investigated the geomagnetic storm event during

17–18 February 1976. This event is characterized by the significant dominance of ~1.0 hour periodicity in the southward component (B_z) of IMF as well as in the electric fields at auroral and dip equatorial stations. On the other hand, *Sastri et al.* [2000] found periodicities in the range of 25–35 min in the *F* region vertical plasma drift (driven by zonal electric field) variations recorded at the nightside dip equatorial ionosphere which are temporally coherent with the variations in B_z of interplanetary magnetic field as well as with the variations in the geomagnetic components. In the present case, however, both the ~1.0 hour and ~0.5 hour periodic components in IEF_y seem to affect the *F* region of the ionosphere over low-equatorial latitudes.

[19] Keeping in mind the possible dependence of the variations in the integrated airglow emission on other factors (like meridional wind) apart from the electric field variations, the causal relationship between the IEF and airglow intensity in the present case is remarkable.

4. Summary

[20] The present investigation elicits the signatures of the solar wind electric field in the OI 630.0 nm airglow recorded at a low-latitude station during a geomagnetic storm event based on the remarkable conformity of small-scale airglow intensity fluctuations with the measurements by three independent (satellite, ionosonde, and magnetometer) techniques. It is found that the periodicities ~0.5 hour and ~1.0 hour in the airglow intensity variations on 12 February 2004 are caused by interplanetary electric field. Further investigations are required to understand the variabilities in the thermospheric airglow emission intensity corresponding to different storm events.

[21] **Acknowledgments.** We would like to thank the ACE SWEPAM and MAG teams as well as ACE Science Center for providing us the ACE data. We thank Indian Institute of Astrophysics for the permission to use the magnetic field data recorded at Hanle. The support provided by the Director, NMRF is duly acknowledged. This work is supported by Department of Space, Government of India.

[22] Arthur Richmond thanks Mangalathayil Abdu and Michael Nicolls for their assistance in evaluating this paper.

References

Barbier, D. (1959), Rsecherches sur la raie 6300 de la luminescence atmospherique nocturne, *Ann. Geophys.*, *15*, 179.

Bittencourt, J. A., and M. A. Abdu (1981), A theoretical comparison between apparent and real vertical ionization drift velocities in the equatorial *F* region, *J. Geophys. Res.*, *86*, 2451.

Chandra, S., E. I. Reed, B. E. Troy Jr., and J. E. Blamont (1973), Equatorial airglow and ionospheric geomagnetic anomaly, *J. Geophys. Res.*, *78*, 4630.

Earle, G. D., and M. C. Kelley (1987), Spectral studies of the sources of ionospheric electric fields, *J. Geophys. Res.*, *92*, 213.

Fejer, B. G., C. A. Gonzales, D. T. Farley, M. C. Kelley, and R. F. Woodman (1979), Equatorial electric fields during magnetically disturbed conditions: 1. The effect of the interplanetary magnetic field, *J. Geophys. Res.*, *84*, 5797.

Gonzales, C. A., M. C. Kelley, B. G. Fejer, J. F. Vickrey, and R. F. Woodman (1979), Equatorial electric fields during magnetically disturbed conditions: 2. Implications of simultaneoues auroral and equatorial mesurements, *J. Geophys. Res.*, *84*, 5803.

Herrero, F. A., and J. W. Meriwether Jr. (1980), 6300A airglow meridional intensity gradients, *J. Geophys. Res.*, *85*, 4191.

Kelley, M. C., J. J. Makela, J. J. Chau, and M. J. Nicollis (2003), Penetration of the solar wind electric field into the magnetosphere/ionosphere system, *Geophys. Res. Lett.*, *30*(4), 1158, doi:10.1029/2002GL016321.

Khan, H., and S. W. H. Cowley (1999), Observations of the response time of high latitude ionospheric convection to variations in the interplanetary magnetic field using EISCAT and IMP-8 data, *Ann. Geophys.*, *17*, 1306.

Kikuchi, T., H. Luhr, T. Kitamura, O. Saka, and K. Schlegal (1996), Direct penetration of the polar electric field to the equator during a DP2 event as detected by the auroral and equatorial magnetometer chains and the EISCAT radar, *J. Geophys. Res.*, *101*, 17,161.

Krishna Murthy, B. V., S. S. Hari, and V. V. Somayajulu (1990), Nighttime equatorial thermospheric meridional winds from ionospheric h′F data, *J. Geophys. Res.*, *95*, 4307.

Kulkarni, P. V., and V. R. Rao (1972), 6300 A night airglow emission over the magnetic equator, *Ann. Geophys.*, *28*, 475.

Lester, M., O. de la Beaujardiere, J. C. Foster, M. P. Freeman, H. Luhr, J. M. Ruohoniemi, and W. Swider (1993), The response of the large scale ionospheric convection pattern to changes in the IMF and substorms: Results from the SUNDIAL 1987 campaign, *Ann. Geophys.*, *11*, 556.

Mendillo, M., and J. Baumgardner (1982), Airglow characteristics of equatorial plasma depletions, *J. Geophys. Res.*, *87*, 7641.

Nishida, A. (1968), Coherence of geomagnetic DP 2 fluctuations with interplanetary magnetic variations, *J. Geophys. Res.*, *73*, 5549.

Peredo, M., J. A. Slavin, E. Majur, and S. A. Curtis (1995), Three dimensional position and shape of the bow shock and their variation with the Alfvenic, sonic and magnetosonic Mach numbers and interplanetary magnetic field orientation, *J. Geophys. Res.*, *100*, 7907.

Reddy, C. A., V. V. Somayajulu, and C. V. Devasia (1979), Global scale electrodynamic coupling of the auroral and equatorial dynamo regions, *J. Atmos. Terr. Phys.*, *41*, 189.

Ridley, A. J., Lu Gang, C. R. Clauer, and V. O. Papitashvili (1998), A statistical study of the ionospheric convection response to changing interplanetary magnetic field conditions using the assimilative mapping of ionospheric electrodynamics technique, *J. Geophys. Res.*, *103*, 4023.

Roelof, E. C., and D. G. Sibeck (1993), Magnetopause shape as a bivariate function of interplanetary magnetic field B_z and solar wind dynamic pressure, *J. Geophys. Res.*, *98*, 21,421.

Sastri, J. H. (2002), Penetration electric fields at the nightside dip equator associated with the main impulse of the storm sudden commencement of 8 July, 1991, *J. Geophys. Res.*, *107*(A12), 1448, doi:10.1029/2002JA009453.

Sastri, J. H., H. Luhr, H. Tachihara, T. I. Kitamura, and J. V. S. V. Rao (2000), Electric field fluctuations (25–35 min) in the midnight dip equatorial ionosphere, *Ann. Geophys.*, *18*, 252.

Schulz, M., and K. Stattegger (1997), Spectrum: Spectral analysis of unevenly spaced paleoclimatic time series, *Comput. Geosci.*, *23*, 929.

Sekar, R., D. Chakrabarty, R. Narayanan, S. Sripathy, A. K. Patra, and K. S. V. Subbarao (2004), Characterizations of VHF radar observations associated with equatorial spread *F* by narrow-band optical measurements, *Ann. Geophys.*, *22*, 3129.

Shirke, J. S. (1963), A comparison of electron density profiles over Ahmedabad in year of low and high solar activity, *J. Atmos. Terr. Phys.*, *25*, 429.

Sobral, J. H. A., M. A. Abdu, C. J. Zamlutti, and I. S. Batista (1980), Association between plasma bubble irregularities and airglow disturbances over Brazilian low latitudes, *Geophys. Res. Lett.*, *7*, 980.

Spreiter, J. R., and S. S. Stahara (1980), A new predictive model for determining solar wind-terrestrial planet interactions, *J. Geophys. Res.*, *85*, 6769.

Sridharan, R., R. Sekar, and S. Gurubaran (1993), Two-dimensional high-resolution imaging of the equatorial plasma fountain, *J. Atmos. Terr. Phys.*, *55*, 1661.

Stening, R. J., and D. E. Winch (1987), Night-time geomagnetic variations at low latitudes, *Planet. Space Sci.*, *35*, 1523.

D. Chakrabarty, R. Sekar, and R. Narayanan, Space and Atmospheric Sciences Division, Physical Research Laboratory, Ahmedabad-380009, Gujarat, India. (dipu@prl.res.in)

C. V. Devasia, Space Physics Laboratory, Vikram Sarabhai Space Center, Thiruvananthapuram-695022, India.

B. M. Pathan, Indian Institute of Geomagnetism, Navi Mumbai-410218, India.